

Article

Simultaneous Mixotrophic Nitrate Removal and Phosphorus Removal in a Sponge-Iron Denitrifying Filter

Xiangyu Sun ^{1,†}, Chunyu Wang ^{1,2,†}, Junbo Zhang ^{1,2}, Zhongtai Chen ^{1,2}, Ting Yu ^{1,2}, Guangjing Xu ^{1,2,3,*} 
and Jingni Xiao ^{1,2,*}

¹ College of Marine Technology and Environment, Dalian Ocean University, Dalian 116023, China; 13865184848@163.com (X.S.)

² Key Laboratory of Nearshore Marine Environmental Science and Technology in Liaoning Province, Dalian Ocean University, Dalian 116023, China

³ Liaoning Provincial Innovation Center for Nearshore Ecological Environment and Disaster Prevention Engineering Technology, Dalian Ocean University, Dalian 116023, China

* Correspondence: xuguangjing@dloou.edu.cn (G.X.); xiaojingni@dloou.edu.cn (J.X.); Tel.: +86-0411-84763287 (G.X.); +86-0411-84762756 (J.X.)

† These authors contributed equally to this work.

Abstract: Due to stricter municipal wastewater discharge standards, there is an increased need for further treatment of nitrate in the secondary effluent of wastewater treatment plants. This is achieved through denitrification by the addition of external carbon sources, which leads to increased costs in wastewater treatment. The aim of this study was to examine the possibility of simultaneous removal of nitrate and phosphorus from simulated secondary effluent by employing a sponge-iron-based denitrifying filter at room temperature. The results indicate that at hydraulic retention times of over 2 h, more than 60% of the nitrate was reduced to ammonia and nitrite via iron-based abiotic nitrate reduction. However, sponge iron easily scaled after two months of operation. Therefore, a little glucose was added to the influent, resulting in a final COD/N ratio of 1:1. Mixotrophic nitrate reduction was observed, and the rust of sponge iron was successfully dissolved. Batch test results demonstrate that biological nitrate denitrification accounted for 70.0% of the total nitrate reduction. Additionally, high-efficiency phosphorus removal through the chemical reaction of released iron and phosphorus was achieved throughout the entire experiment, with removal efficiencies of more than 90% at hydraulic retention times of over 2 h. Moreover, high-throughput sequencing data show that the species diversity obviously increased after adding organic carbon, suggesting the coexistence of heterotrophic and autotrophic denitrifiers. Hence, the sponge-iron denitrifying filter has considerable prospects in the field of secondary effluent treatment and is likely to be the future direction of zero-valent iron application in sewage treatment.

Keywords: sponge iron; autotrophic denitrification; municipal wastewater; chemical phosphorus removal



Citation: Sun, X.; Wang, C.; Zhang, J.; Chen, Z.; Yu, T.; Xu, G.; Xiao, J. Simultaneous Mixotrophic Nitrate Removal and Phosphorus Removal in a Sponge-Iron Denitrifying Filter. *Water* **2023**, *15*, 2248. <https://doi.org/10.3390/w15122248>

Academic Editor: Saglara S. Mandzhieva

Received: 10 May 2023

Revised: 12 June 2023

Accepted: 13 June 2023

Published: 15 June 2023



Copyright: © 2023 by the authors. Licensee MDPI, Basel, Switzerland. This article is an open access article distributed under the terms and conditions of the Creative Commons Attribution (CC BY) license (<https://creativecommons.org/licenses/by/4.0/>).

1. Introduction

With the improvement of China's urban sewage discharge standards, many wastewater treatment plants need to upgrade and retrofit their facilities to meet more stringent pollutant discharge standards (GB-18918—2002 Class A) [1,2]. In general, it is difficult to meet the total nitrogen (TN) discharge standards (i.e., the effluent TN limit is 15 mg/L), reflecting the high nitrate residues due to insufficient organic carbon in the municipal wastewater [3]. As a result, denitrifying filters (DNFs) are commonly used to remove nitrate from the secondary effluent [4]. Generally, traditional DNF processes are greatly affected by temperature, the COD/N ratio, type of organic carbon source, and biofilm thickness [5]. In particular, the efficiency of denitrification in the DNF is severely restricted by the COD/N ratio, and external carbon sources, such as glucose, acetate, methanol,

ethanol etc., need to be supplemented to improve the denitrification efficiency of the DNF system. This, however, increases the cost of wastewater treatment and the amount of waste sludge generated [6,7]. To tackle the high costs and unsustainability of traditional heterotrophic denitrification, researchers have explored autotrophic denitrification as a potential solution. Autotrophic denitrification uses microorganisms that can convert nitrate to nitrogen gas without an external carbon source, making it a more cost-effective and sustainable alternative. Commonly, the electron donors of autotrophic denitrification are the sulfur, hydrogen, and iron compounds, thiosulphate and reduced iron [8]. Iron autotrophic denitrification is a biological nitrate removal process that utilizes iron (Fe^0) or ferrous ions (Fe^{2+}) as electron donors [9]. This process requires little oxygen and organic matter, and is completely different from the conventional heterotrophic denitrification in wastewater treatment plants. Although certain amounts of iron metals are needed for nitrate removal, the resulting byproduct of ferric ion reacts with phosphorus, forming ferric phosphate, and thereby removes phosphorus from the wastewater [10]. Furthermore, the formed $\text{Fe}(\text{OH})_3$ facilitates phosphorus removal by adsorbing it [11]. Additionally, it is well known that iron is cheaper and more readily available than organic matter. Therefore, reduced iron serves not only as an electron donor for nitrate reduction but also as an efficacious phosphorus removal agent [12]. Remarkably, the released iron functions as a trace element that also stimulates microbial metabolic activity [13]. However, zero-valent iron, which is commonly used in this process, can easily form iron oxides on its surface under high pH conditions, which can compromise the further reduction of nitrate by obstructing the active sites on the surface of the iron particles and its electron release [14]. To address this issue, reducing agents or assistants can be added to the denitrification filters to help prevent the formation of iron oxides. The reducing agents work by creating a reducing environment that counteracts the oxidative environment that promotes iron oxide formation. As a result, the reducing agents help to maintain the integrity of the zero-valent iron particles, and prevent the scaling problems that can occur in denitrification filters.

Rust is a common term used to describe the corrosion of iron or steel that occurs when they are exposed to oxygen and moisture in the environment. Iron-reducing bacteria have been found to be capable of dissolving rust in the presence of organic matter. Iron-reducing bacteria are a group of microorganisms that are able to use iron as an electron acceptor in their metabolism, which can cause significant alterations through anaerobic respiration, resulting in the degradation of organic matter and iron reduction [15]. Iron oxides serve as electron acceptors for iron-reducing bacteria, and the products mainly include magnetite (Fe_3O_4), siderite (FeCO_3), vivianite ($\text{Fe}_3(\text{PO}_4)_2 \cdot 8 \text{H}_2\text{O}$), green rust, and soluble Fe^{2+} [16]. In addition, many microbes are capable of coupling iron oxidation to denitrification under mixotrophic conditions, where acetate is the most effective organic electron donor enhancing denitrification rates [17]. As such, combined heterotrophic denitrification and nitrate-dependent Fe (II) oxidation is a promising biotechnology to be employed for the dissolution of iron oxides on the surface of iron biocarriers. However, acetate is a simple carbon source that can be utilized directly by organisms and plays a significant role in rusting iron [17]. In contrast, complex organic carbon matter undergoes hydrolysis in the wastewater and releases short-chain fatty acid ions around the cell [18], creating a local acidic environment that may dissolve rust, but this requires further verification. In any case, high-efficiency nitrogen removal could be achieved via mixotrophic denitrification in the presence of organic carbon and iron particles. More importantly, mixotrophic denitrification requires less organic matter, which helps save resources and reduces environmental impacts compared with heterotrophic denitrification. Additionally, compared with autotrophic denitrification, mixotrophic denitrification can be started in a shorter time and has a higher removal efficiency, making it suitable for many environments with harsh natural conditions [19].

Therefore, this study aimed to develop a DNF using sponge iron as a biocarrier to identify the feasibility of simultaneous mixotrophic nitrate removal and chemical phosphorus removal from a simulated secondary effluent. The contributions of biological nitrogen

removal and iron-based autotrophic denitrification were analyzed through batch tests. High-throughput sequencing techniques were utilized to analyze the functional genes of microorganisms involved in mixotrophic denitrification at different stages of the experiment. Additionally, heterotrophic denitrification for rusted iron renewal is also explored in this study.

2. Materials and Methods

2.1. Experimental Equipment

The experiment was carried out in a DNF using sponge iron (5–7 mm) as a filter and biofilm carrier (Figure 1). The height and diameter of the sponge-iron layer was 16 cm and 8 cm, respectively. The sponge iron accounted for about 70% of the total DNF volume. The influent wastewater entered into the bottom of the DNF at different flow rates of 4 cm/h, 8 cm/h, 16 cm/h, and 32 cm/h, leading to different hydraulic retention times (HRT), namely, 4 h, 2 h, 1 h, and 0.5 h, respectively. The experiment was divided into three stages based on the HRT and other operational conditions. During Stage I, which lasted from day 1 to day 41, the HRT was reduced gradually from 4 h to 1 h. In Stage II, which lasted from day 42 to day 73, the HRT was increased from 1.5 h to 3 h. During Stage III, which lasted from day 74 to day 100, the HRT was set to 4 h. The temperature during the experiment was maintained at room temperature.

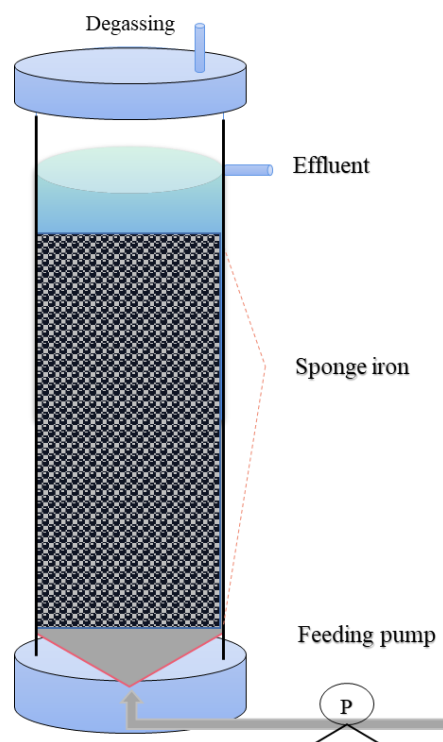


Figure 1. Diagram of iron-based denitrifying filter.

The influent composition for the experiment primarily consisted of NO_3^- -N at a concentration of 10 mg/L, and small amounts of micronutrient elements, including MgSO_4 (10 mg/L), CaCl_2 (20 mg/L), EDTA (20 mg/L), and NaH_2PO_4 (20 mg/L). During the startup period of the DNF, no activated sludge was seeded. On the 14th day, the influent PO_4^{3-} -P concentration of the DNF was adjusted from 2.5 mg/L to 5 mg/L in order to increase the TP (total phosphorus) operating load. Then, on the 82nd day, glucose was introduced into the influent of the DNF, resulting in a final COD/N ratio of 1:1. In addition, the DNF was washed using potable water once per week.

2.2. Batch Tests

To determine the nitrate removal pathway in the DNF, batch tests were carried out in three wide-mouth bottles on the 85th day in Stage III. The test comprised three groups. The first group contained new sponge iron, the second contained sponge iron with biofilm from the DNF system, and the third contained sponge iron with inactivated DNF biofilm heated at 100 °C for 30 min. A similar amount of sponge iron with biofilm was collected and cleaned for the test. For the batch test, a synthetic wastewater with glucose and nitrate was prepared with a COD/N ratio of 1:1 and pH of 7.0. The temperature was maintained at 28 °C to obtain high bacterial activity in a self-heated laboratory water bath, and samples were taken at different time intervals (0.5 h, 1 h, 1.5 h, and 2 h) to measure the levels of NH_4^+ -N, NO_2^- -N and NO_3^- -N after filtration with 0.22- μm filters. The mixing was performed using pure nitrogen gas during the whole batch test.

To investigate the recovery of denitrification in sponge iron after adding glucose as a carbon source, a batch experiment was conducted in the DNF system. The sponge iron experienced a high loss of activity after operating for a long time. To clean the sponge iron carriers, they were rinsed three times, and a simulated wastewater with a COD/N ratio of 1:1 was introduced once. In the batch experiment, the inlet pipe was placed in the clean water zone and operated in recirculating mode. The water temperature was about 18 °C (room temperature).

2.3. Analytical Methods

NH_4^+ -N, NO_2^- -N, NO_3^- -N, and COD were determined according to standard methods [20]. Total inorganic nitrogen (TIN) was a sum of inorganic NH_4^+ -N, NO_2^- -N and NO_3^- -N.

The bacterial community in a biofilm was studied using a high-throughput sequencing method. Sludge samples were collected on the 57th day (Stage II) and 88th day (Stage III), respectively. DNA was extracted using the E.Z.N.A™ Fast DNA Spin Kit from OMEGA, and PCR was carried out using an ETC Thermocycler from Innovation Biotech in Beijing, China. The V3-V4 regions of bacterial 16 S rRNA genes were amplified using the Nobar_341 F and Nobar_805 R primer set. The resulting amplicons were sequenced using the MiSeq system (Sangon Biotech, Shanghai, China).

3. Results and Discussion

3.1. Nitrogen Transformation in the Sponge-Iron-Based DNF

During the first stage of operation, the concentration of NO_3^- -N in the effluent remained consistently below 0.5 mg/L during the initial 14 days, with an impressive average nitrate removal rate of 98.7% (Figure 2A). No activated sludge was seeded, and as a result, nitrate was primarily removed through chemical reactions [15]. Long HRT allowed for an adequate time for chemical reactions to occur within the reactor (as described by Equations (1)–(3)). Although the accumulated concentration of NO_2^- -N only averaged around 0.35 ± 0.31 mg/L, the highest observed concentration of NH_4^+ -N in the effluent was 7.19 ± 0.32 mg/L, which was due to the reaction described by Equation (4), and only Fe^0 was involved this reaction at a long HRT and high iron-to-nitrate ratio [21]. Indeed, there was little biomass attached to the iron surface during this initial stage, so NO_3^- -N could adequately come into contact with the iron, resulting in a high nitrate reduction efficiency, especially at longer HRTs. Further calculations suggested that approximately 7.5 mg/L of NO_3^- -N was consumed, with a little NO_3^- -N being converted to N_2 and emitted from the DNF (as shown in Equation (3)). As such, nitrate was mostly reduced to ammonium using iron as an electron donor, without seeding activated sludge in the initial period. This led to high ammonium production and low TIN removal efficiency (Figure 2B).



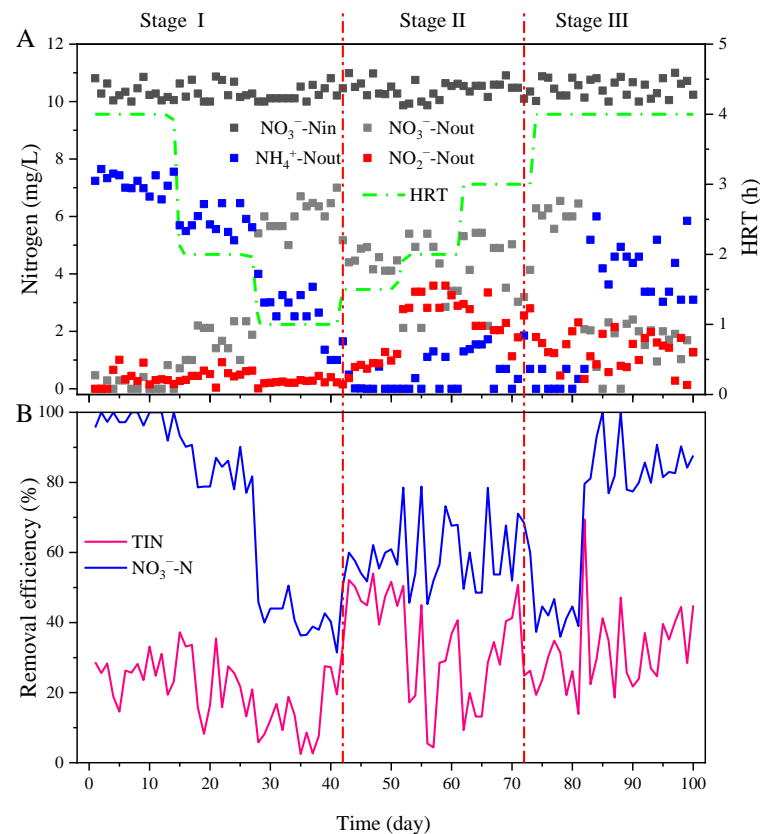
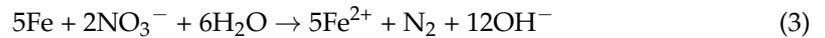


Figure 2. Denitrification of the DNF at different HRT. (A) Nitrogen concentration profiles at different HRT; (B) TIN and nitrate removal efficiency.

Figure 2A also shows that between the 15th and 27th day of operation, the HRT was reduced to 2 h, resulting in an effluent NO_3^- -N concentration of approximately 1.37 ± 0.78 mg/L. During this period, the NO_3^- -N removal efficiency was approximately 86.8%, and the NH_4^+ -N concentration decreased to 5.82 ± 0.41 mg/L, while the effluent NO_2^- -N remained at 0.48 ± 0.21 mg/L. It was during this time that the activity of iron-based autotrophic denitrifying bacteria probably had a more pronounced effect. From the 28th to the 42nd day of the operation, the HRT further decreased to 1 h, and the NO_3^- -N removal efficiency significantly dropped to 41.6%. In addition, the effluent NH_4^+ -N concentration decreased to 2.62 ± 0.92 mg/L, while the NO_2^- -N concentration remained at around 0.25 ± 0.10 mg/L. Therefore, the nitrate reduction was highly affected by the shortening of HRT.

The TIN removal efficiency was always lower than 40%, especially at short HRTs (Figure 2B). During Stage II, the HRT was then adjusted to 1.5 h between days 42 and 51. As a result, the NO_3^- -N removal efficiency recovered to 58.9%. Additionally, only a small amount of NH_4^+ -N (0.29 ± 0.07 mg/L) and NO_2^- -N (0.81 ± 0.34 mg/L) accumulated in the effluent, and the average TIN removal efficiency reached 48.4%. It was observed that the TIN removal efficiency was the best during this period. In addition, the accumulated level of NO_2^- -N was also high during this period. Surprisingly, the effluent NH_4^+ -N

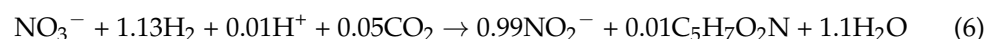
was almost under the detection limit. This could be attributed to the excessive growth of algae biofilm in the presence of sunlight, which might absorb the accumulated $\text{NH}_4^+\text{-N}$ through photosynthesis, while the oxygen generated by algae was used for ammonium oxidization to nitrite by ammonium-oxidizing bacteria [22–24]. This hypothesis requires further investigation before it can be confirmed.

During days 52–73 of the experiment, shading was used to prevent the negative impact of algae growth in the DNF system. Despite gradually increasing the HRT to 3 h, the removal efficiency of $\text{NO}_3^-\text{-N}$ remained at 64.4%. This was likely due to scaling on the iron surface, which was visibly rusted during this period. Without algal N-assimilation due to the absence of light, the concentration of $\text{NH}_4^+\text{-N}$ in the effluent also increased to 0.71 ± 0.67 mg/L. Furthermore, nitrite accumulation in the effluent increased, with an average concentration of 2.34 ± 0.59 mg/L. The generation of $\text{NO}_2^-\text{-N}$ was possibly due to heterotrophic denitrification, which utilized organic carbon released from algae decomposition as a carbon source, or autotrophic denitrification using hydrogen generated from iron corrosion [25].

During days 74 to 82 of Stage III, the HRT was extended to 4 h, but the average nitrate removal efficiency decreased to 49.1%. The effluent $\text{NH}_4^+\text{-N}$ and $\text{NO}_2^-\text{-N}$ slightly decreased with average concentrations of 0.27 ± 0.34 mg/L and 1.40 ± 0.66 mg/L, respectively. This suggests that there was insufficient supply of electron donors due to iron scaling and lack of organic carbon. Glucose was subsequently added to the influent from the 83rd day onwards, resulting in a low COD/N ratio of 1:1 and a significant decrease in the effluent $\text{NO}_3^-\text{-N}$ concentration. The average $\text{NO}_3^-\text{-N}$ removal efficiency increased to 85.2%, while the effluent $\text{NH}_4^+\text{-N}$ and $\text{NO}_2^-\text{-N}$ increased to 4.27 ± 0.94 mg/L and 1.25 ± 0.60 mg/L, respectively. This indicates that the iron rust was dissolved after glucose addition [17]. Importantly, a stable mixotrophic denitrification process was established, also enabled by stable iron release in the presence of organic carbon.

3.2. Autotrophic and Heterotrophic Denitrifying Activity in the DNF

On the 85th day, an experiment was conducted to investigate the autotrophic and heterotrophic denitrifying activity in the DNF. The results are presented in Figure 3, which shows that the nitrate removal rate was 1.22, 3.44, and 1.03 mg/(L·h) in the new sponge iron, DNF iron and live biofilm, and DNF iron and dead biofilm, respectively. Based on calculations, it was found that biological nitrate reduction accounted for 70.0% of the total nitrate reduction. Therefore, it was concluded that the iron-based nitrate reduction activities were significantly lower than biological denitrification activity in the presence of glucose, but some Fe^0 , Fe^{2+} and hydrogen generated by iron corrosion was used for denitrification by biological pathways [26,27]. In the activated sludge system, a complex mixture of molecules, ions and biological enzymes coexist, leading to a complex reaction process. Equations (5)–(7) represent some of the possible reactions that can occur in this system. Of these, Equations (6) and (7) are performed in living organisms, e.g., denitrifying bacteria.



After obvious iron corrosion was observed on the surface of sponge iron particles, glucose was added to the DNF system, which resulted in the promotion of heterotrophic denitrifying bacteria. It further accelerated the dissolution of iron rust and thereby restored the reduction of internal iron. The batch experiments demonstrated that the iron reduction activity of the restored DNF biocarriers improved significantly after recovery. Figure 4 shows that 50.2% of the nitrate was removed and there was a noticeable accumulation of ammonia. From the 60th min onwards, ammonium concentration increased to about

2 mg/L, while the nitrite concentration remained at 0 mg/L, which demonstrates that all the ammonium produced by iron-based nitrate reduction (Equation (4)) accumulated in the DNF without oxygen. While there was also an observed removal of TIN, the activity was slightly low due to the operation temperature being low. Moreover, the phosphorus removal rate reached an impressive 94.6%, which indicates successful recovery of iron release after promoting heterotrophic denitrification. Iron-reducing bacteria can help dissolve the rust on the sponge-iron surface by facilitating the transfer of electrons between the iron and the bacteria, which allows the iron to continue to release iron ions and further aids in the reduction of rust [16]. Consequently, the addition of glucose proved to be an effective solution to the issue of iron scaling.

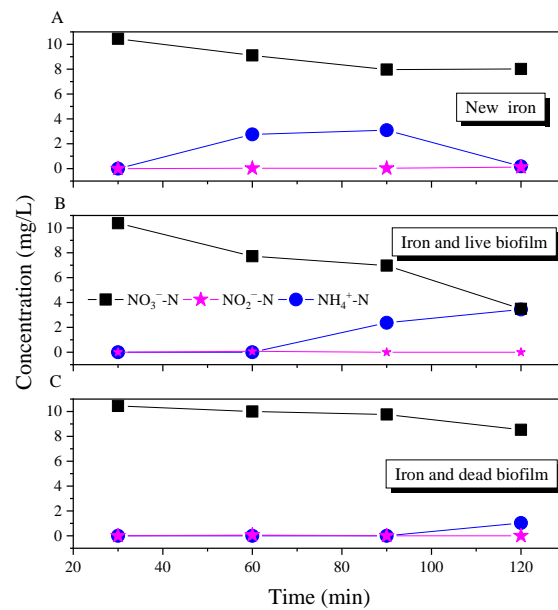


Figure 3. Activity of biological and/or chemical denitrification. (A) new sponge iron; (B) sponge iron with live biofilm; (C) sponge iron with dead biofilm.

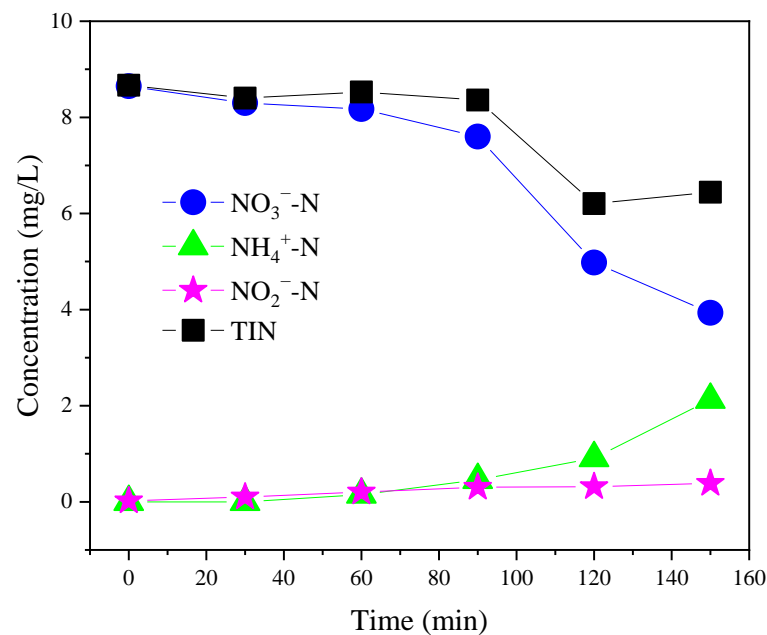


Figure 4. Nitrate transformation activity of the DNF after adding glucose.

3.3. Chemical Phosphorus Removal in the Sponge-Iron-Based DNF

Figure 5 shows the concentration profiles of phosphorus in the DNF. During the initial 14 days, nearly all of the phosphorus was removed. The main reason was that the influent load was small, and many iron ions were released from the sponge iron via Equations (3) and (4) at a long HRT of 4 h. Phosphorus reacted with iron ions to generate iron-phosphate precipitation or was absorbed by colloidal $\text{Fe}(\text{OH})_3$ (Equations (8) and (9)).

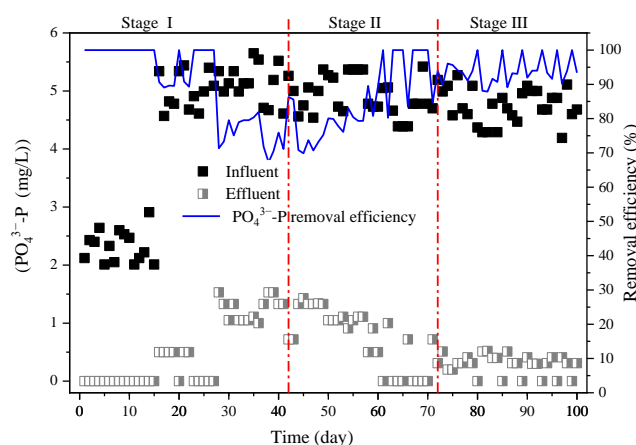


Figure 5. Concentration profiles of phosphorus in the DNF.

During days 15–27, with an HRT of 2 h and an influent phosphorus concentration of about 5.0 mg/L, the average efficiency of phosphorus removal reached as high as 94.9%. As the HRT was reduced to 1–1.5 h during days 28–51, the phosphorus removal efficiency decreased to about 76.0%, indicating that the released iron ions were insufficient for phosphorus removal at short HRTs, which could reflect the decreasing iron-based nitrate reduction with shortening HRT. During days 52–61, when the HRT was increased back to 2 h, the average efficiency of phosphorus removal increased to 83.6%. During days 62–73 with an HRT of 3 h, the average efficiency of phosphorus removal increased to about 94.4%. During days 74–100 with an HRT of 4 h, the average efficiency of phosphorus removal increased to about 95.1%. Therefore, HRT played a critical role in the phosphorus removal of an iron-based DNF, while 3 h was beneficial for phosphorus removal.

3.4. Microbial Community Composition

The results above show that strong biological nitrogen transformation was observed in the DNF. The high-throughput sequencing results in Figure 6 show that the dominant phylum in both stages was Proteobacteria, while its abundance in Stage II (72.4%) was far higher than in Stage III (49.6%). Actinobacteria abundance also decreased from 14.8% to 8.5%. The abundance of Cyanobacteria-Chloroplast in Stage III (21.0%) was significantly higher than in Stage II (4.1%), which could be attributed to the growth of algae in the DNF. Furthermore, the phyla Planctomycetes, Armatimonadetes and Chloroflexi were obviously enriched in Stage III due to addition of glucose.

At the family level, the species diversity was much greater at Stage III of the DNF, especially for families that accounted for more than 1% of the total bacteria, which were much more abundant than those in Stage II. However, in Stage III, the abundance of Xanthomonadaceae, Mycobacteriaceae, Pseudomonadaceae and Caulobacteraceae greatly decreased. The family Xanthomonadaceae contains autotrophic denitrifiers that use iron as an electron donor, such as the genus *Thermomonas* [28]. However, the percentage of *Thermomonas*

decreased from 9.7% in Stage II to 7.2% in Stage III with the addition of glucose, suggesting that iron-based autotrophic denitrifiers were easily outcompeted by heterotrophic denitrifiers in the presence of organics [29]. The long-term performance and batch test results also confirmed that iron-based denitrification was inhibited by heterotrophic denitrification, but iron-based autotrophic denitrifiers and heterotrophic denitrifiers could coexist at low COD/N ratios, such as 1:1 in this study. In addition, microbial activity could be enhanced by iron ions [26,30]. Additionally, the family Comamonadaceae, which primarily consists of the genus *Hydrogenophaga*, a group of autotrophic bacteria that oxidize hydrogen [31], experienced a decrease from 3.3% in Stage II to 2.4% in Stage III due to competition with heterotrophic denitrifiers for nitrate.

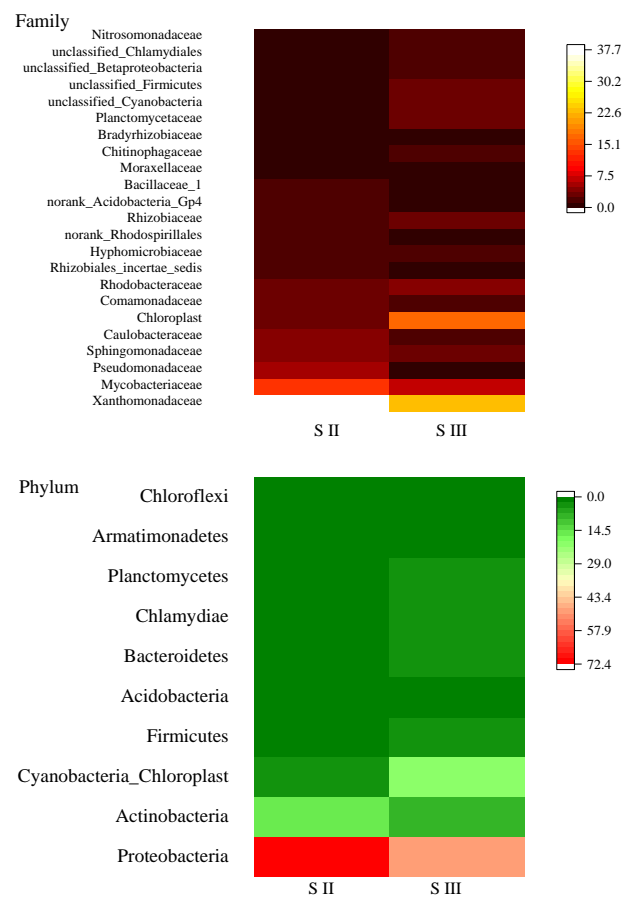


Figure 6. Comparison of bacterial composition between Stages II and III at phylum and family level.

In fact, *Aquimonas*, which is possibly responsible for nitrification [24], was the most dominant genus in both Stages II and III, with an abundance of 27.5% and 18.5%, respectively. Although the abundance of *Aquimonas* decreased, the abundance of *Nitrosomonas*, a common ammonium-oxidizing bacteria [23], increased in Stage III. In addition, many *Chloroplast* were also observed in both Stage II (3.4%) and III (17.3%), which supports the best TIN removal occurred in Stage II rather than Stage III. This was because the produced ammonium was mainly oxidized by nitrifiers, which were outcompeted by heterotrophic bacteria in the presence of organics [32]. Moreover, the families Rhizobiaceae, Parachlamydiaceae, Planctomycetaceae, as well as some Cyanobacteria, Firmicutes, Betaproteobacteria, and Alphaproteobacteria greatly increased. Therefore, after organic matter was added, heterotrophic bacteria, including heterotrophic denitrifying bacteria, required an electron donor for their growth and metabolism. Iron-reducing bacteria could also obtain a certain number of electrons to reduce high-valence iron and release iron ions, which promoted the conversion of nitrogen and organic carbon by more bacteria and microalgae. Meanwhile, after the rust was removed, zero-valent iron became active and underwent denitrification,

accompanied by ammonia nitrogen enrichment, which provided a better growth environment for ammonia-oxidizing bacteria and algae. These results suggest that the addition of organic matter significantly increased the biodiversity of the DNF system using sponge-iron as biocarriers.

4. Conclusions

In this study, the potential of sponge-iron DNF in treating stimulated secondary effluent was investigated. The study found that the iron-based autotrophic denitrification process was significantly affected by hydraulic retention time HRT. At longer HRTs (over two hours), chemical iron-based denitrification converted most of the nitrate to ammonium during the initial stage. As a biofilm developed on the surface of the sponge iron, nitrite became the primary reduction product in the DNF effluent. Furthermore, batch tests revealed that about 70% of the nitrate reduction was achieved through a biological pathway. However, the efficiency of nitrate reduction decreased considerably after running the DNF for around two months, possibly due to the scaling of sponge iron. Consequently, the removal efficiency of both nitrogen and phosphorus dropped. To overcome this issue, glucose was added to the influent of the DNF, leading to a rapid increase in nitrate removal efficiency due to the coexistence of mixotrophic nitrate reduction, which was demonstrated by an increase in the DNF's biodiversity. In addition, the phosphorus removal efficiency improved significantly. Overall, this study suggests that sponge-iron DNF technology could remove both nitrate and phosphorus, allowing the treatment of municipal wastewater without relying on external carbon sources for deep nitrogen removal and chemicals for phosphorus removal, thus saving operational costs.

Author Contributions: Methodology, C.W.; Validation, X.S.; Formal analysis, T.Y.; Resources, Z.C.; Data curation, J.Z.; Writing—original draft, X.S. and C.W.; Writing—review & editing, G.X. and J.X.; Supervision, G.X. and J.X.; Funding acquisition, G.X. All authors have read and agreed to the published version of the manuscript.

Funding: This research was funded by Major Science and Technology Projects of Liaoning Province (No. 2020 JH1/10200002) and the scientific research project of the Department of Education of Liaoning province (LJKMZ20221122).

Data Availability Statement: The data are contained within the article.

Conflicts of Interest: The authors declare no conflict of interest.

References

1. Wei, Z.; He, Y.; Wang, X.; Chen, Z.; Wei, X.; Lin, Y.; Cao, C.; Huang, M.; Zheng, B. A comprehensive assessment of upgrading technologies of wastewater treatment plants in Taihu Lake Basin. *Environ. Res.* **2022**, *212*, 113398. [[CrossRef](#)]
2. Cao, Y.; Van Loosdrecht, M.C.M.; Daigger, G.T. The bottlenecks and causes, and potential solutions for municipal sewage treatment in China. *Water Pract. Technol.* **2020**, *15*, 160–169. [[CrossRef](#)]
3. Zhong, L.; Yang, S.-S.; Ding, J.; Wang, G.-Y.; Chen, C.-X.; Xie, G.-J.; Xu, W.; Yuan, F.; Ren, N.-Q. Enhanced nitrogen removal in an electrochemically coupled biochar-amended constructed wetland microcosms: The interactive effects of biochar and electrochemistry. *Sci. Total Environ.* **2021**, *789*, 147761. [[CrossRef](#)]
4. Li, P.; Zuo, J.; Wang, Y.; Zhao, J.; Tang, L.; Li, Z. Tertiary nitrogen removal for municipal wastewater using a solid-phase denitrifying biofilter with polycaprolactone as the carbon source and filtration medium. *Water Res.* **2016**, *93*, 74–83. [[CrossRef](#)] [[PubMed](#)]
5. Wu, L.; Wei, W.; Xu, J.; Chen, X.; Liu, Y.; Peng, L.; Wang, D.; Ni, B.-J. Denitrifying biofilm processes for wastewater treatment: Developments and perspectives. *Environ. Sci. Water Res. Technol.* **2021**, *7*, 40–67. [[CrossRef](#)]
6. Fu, X.; Hou, R.; Yang, P.; Qian, S.; Feng, Z.; Chen, Z.; Wang, F.; Yuan, R.; Chen, H.; Zhou, B. Application of external carbon source in heterotrophic denitrification of domestic sewage: A review. *Sci. Total Environ.* **2022**, *817*, 153061. [[CrossRef](#)] [[PubMed](#)]
7. Zhou, T.; Liu, J.; Lie, Z.; Lai, D.Y.F. Effects of applying different carbon substrates on nutrient removal and greenhouse gas emissions by constructed wetlands treating carbon-depleted hydroponic wastewater. *Bioresour. Technol.* **2022**, *357*, 127312. [[CrossRef](#)] [[PubMed](#)]
8. Zhang, J.; Fan, C.; Zhao, M.; Wang, Z.; Jiang, S.; Jin, Z.; Bei, K.; Zheng, X.; Wu, S.; Lin, P.; et al. A comprehensive review on mixotrophic denitrification processes for biological nitrogen removal. *Chemosphere* **2023**, *313*, 137474. [[CrossRef](#)]

9. Chen, S.; Zhou, B.; Chen, H.; Yuan, R. Iron mediated autotrophic denitrification for low C/N ratio wastewater: A review. *Environ. Res.* **2023**, *216*, 114687. [[CrossRef](#)]
10. Tian, T.; Zhou, K.; Li, Y.-S.; Liu, D.-F.; Yu, H.-Q. Phosphorus Recovery from Wastewater Prominently through a Fe(II)-P Oxidizing Pathway in the Autotrophic Iron-Dependent Denitrification Process. *Environ. Sci. Technol.* **2020**, *54*, 11576–11583. [[CrossRef](#)] [[PubMed](#)]
11. Na, C.-K.; Park, G.-Y.; Park, H.J. Applicability of ferric(III) hydroxide as a phosphate-selective adsorbent for sewage treatment. *Water Sci. Technol.* **2021**, *83*, 2911–2920. [[CrossRef](#)] [[PubMed](#)]
12. Bai, Y.; Wang, S.; Zhussupbekova, A.; Shvets, I.V.; Lee, P.-H.; Zhan, X. High-rate iron sulfide and sulfur-coupled autotrophic denitrification system: Nutrients removal performance and microbial characterization. *Water Res.* **2023**, *231*, 119619. [[CrossRef](#)]
13. You, G.; Wang, C.; Hou, J.; Wang, P.; Xu, Y.; Miao, L.; Liu, J. Effects of zero valent iron on nitrate removal in anaerobic bioreactor with various carbon-to-nitrate ratios: Bio-electrochemical properties, energy regulation strategies and biological response mechanisms. *Chem. Eng. J.* **2021**, *419*, 129646. [[CrossRef](#)]
14. Liu, Y.; Wang, J. Reduction of nitrate by zero valent iron (ZVI)-based materials: A review. *Sci. Total Environ.* **2019**, *671*, 388–403. [[CrossRef](#)] [[PubMed](#)]
15. Fan, Y.-Y.; Li, B.-B.; Yang, Z.-C.; Cheng, Y.-Y.; Liu, D.-F.; Yu, H.-Q. Abundance and diversity of iron reducing bacteria communities in the sediments of a heavily polluted freshwater lake. *Appl. Microbiol. Biotechnol.* **2018**, *102*, 10791–10801. [[CrossRef](#)]
16. Starosvetsky, J.; Kamari, R.; Farber, Y.; Bilanović, D.; Armon, R. Rust dissolution and removal by iron-reducing bacteria: A potential rehabilitation of rusted equipment. *Corros. Sci.* **2016**, *102*, 446–454. [[CrossRef](#)]
17. Kiskira, K.; Papirio, S.; van Hullebusch, E.D.; Esposito, G. Fe(II)-mediated autotrophic denitrification: A new bioprocess for iron bioprecipitation/biorecovery and simultaneous treatment of nitrate-containing wastewaters. *Int. Biodeterior. Biodegrad.* **2017**, *119*, 631–648. [[CrossRef](#)]
18. Dhamole, P.B.; D'Souza, S.F.; Lele, S.S. A Review on Alternative Carbon Sources for Biological Treatment of Nitrate Waste. *J. Inst. Eng. (India) Ser. E* **2015**, *96*, 63–73. [[CrossRef](#)]
19. Abu Hasan, H.; Muhammad, M.H.; Ismail, N.I. A review of biological drinking water treatment technologies for contaminants removal from polluted water resources. *J. Water Process Eng.* **2020**, *33*, 101035. [[CrossRef](#)]
20. APHA. *Standard Methods for the Examination of Water and Wastewater*; American Public Health Association: Washington, DC, USA, 1998.
21. Huang, C.-P.; Wang, H.-W.; Chiu, P.-C. Nitrate reduction by metallic iron. *Water Res.* **1998**, *32*, 2257–2264. [[CrossRef](#)]
22. Rana, M.S.; Prajapati, S.K. Resolving the dilemma of iron bioavailability to microalgae for commercial sustenance. *Algal Res.* **2021**, *59*, 102458. [[CrossRef](#)]
23. Arp, D.J.; Sayavedra-Soto, L.A.; Hommes, N.G. Molecular biology and biochemistry of ammonia oxidation by *Nitrosomonas europaea*. *Arch. Microbiol.* **2002**, *178*, 250–255. [[CrossRef](#)] [[PubMed](#)]
24. Li, L.; Zhang, B.; Shi, J.; He, J.; Zhang, W.; Yan, W.; Li, M.; Tang, C.; Li, H. Concurrent vanadate and ammonium abatement in a membrane biofilm reactor. *Chem. Eng. J.* **2022**, *442*, 136285. [[CrossRef](#)]
25. Wang, Z.; Wang, H.; Ma, L. Iron shavings supported biological denitrification in sequencing batch reactor. *Desalination Water Treat.* **2012**, *49*, 95–105. [[CrossRef](#)]
26. Chen, H.; Zhao, X.; Cheng, Y.; Jiang, M.; Li, X.; Xue, G. Iron Robustly Stimulates Simultaneous Nitrification and Denitrification Under Aerobic Conditions. *Environ. Sci. Technol.* **2018**, *52*, 1404–1412. [[CrossRef](#)]
27. Peng, L.; Liu, Y.; Gao, S.-H.; Chen, X.; Xin, P.; Dai, X.; Ni, B.-J. Evaluation on the Nanoscale Zero Valent Iron Based Microbial Denitrification for Nitrate Removal from Groundwater. *Sci. Rep.* **2015**, *5*, 12331. [[CrossRef](#)]
28. Torrentó, C.; Urmeneta, J.; Otero, N.; Soler, A.; Viñas, M.; Cama, J. Enhanced denitrification in groundwater and sediments from a nitrate-contaminated aquifer after addition of pyrite. *Chem. Geol.* **2011**, *287*, 90–101. [[CrossRef](#)]
29. Shi, Y.; Liu, T.; Yu, H.; Quan, X. Enhancing anoxic denitrification of low C/N ratio wastewater with novel ZVI composite carriers. *J. Environ. Sci.* **2022**, *112*, 180–191. [[CrossRef](#)]
30. Lu, J.s.; Lian, T.t.; Su, J.f. Effect of zero-valent iron on biological denitrification in the autotrophic denitrification system. *Res. Chem. Intermed.* **2018**, *44*, 6011–6022. [[CrossRef](#)]
31. Suzuki, S.; Kuenen, J.G.; Schipper, K.; van der Velde, S.; Ishii, S.i.; Wu, A.; Sorokin, D.Y.; Tenney, A.; Meng, X.; Morrill, P.L.; et al. Physiological and genomic features of highly alkaliphilic hydrogen-utilizing Betaproteobacteria from a continental serpentinizing site. *Nat. Commun.* **2014**, *5*, 3900. [[CrossRef](#)]
32. Navada, S.; Knutsen, M.F.; Bakke, I.; Vadstein, O. Nitrifying biofilms deprived of organic carbon show higher functional resilience to increases in carbon supply. *Sci. Rep.* **2020**, *10*, 7121. [[CrossRef](#)] [[PubMed](#)]

Disclaimer/Publisher's Note: The statements, opinions and data contained in all publications are solely those of the individual author(s) and contributor(s) and not of MDPI and/or the editor(s). MDPI and/or the editor(s) disclaim responsibility for any injury to people or property resulting from any ideas, methods, instructions or products referred to in the content.